Master of Science

The Size Effect on Chemical Interface Damping of Single Gold Nanorods and Its Application to Biosensing

The Graduate School of the University of Ulsan

Department of Chemistry

Seong Woo Moon

The Size Effect on Chemical Interface Damping of Single Gold Nanorods and Its Application to Biosensing

Supervisor: Ji Won Ha

A Dissertation

Submitted to

The Graduate School of the University of Ulsan

In partial fulfillment of the requirements

for the degree of

Master of Science in Department of Chemistry

by

Seong Woo Moon

University of Ulsan, Ulsan, Korea, 2009

January, 2019

The Size Effect on Chemical Interface Damping of Single Gold Nanorods and Its Application to Biosensing

This certifies that the dissertation of Seong Woo Moon is approved.

Committee	Ji Won Ha
Committee	Youngil Lee
Committee	Yong Soo Kim

Department of Chemistry

Ulsan, Korea

January, 2019

국문 초록

금속 나노 입자 중 금, 은, 구리와 같은 귀금속 나노 입자는 독특한 광학적 특성으로 인해 다양한 분야에서 응용되고 있다. 특히 금 나노 입자(gold nanoparticle, AuNP)의 경우 국지 표면 플라즈몬 공명(localized surface plasmon resonance, LSPR)을 기반으로 한 센서분야에 많이 연구되어지고 있다. 다양한 모양의 금 나노 입자 중에서도 막대모양 입자의 경우 비등방성 모양을 가지고 있어 굴절률 기반의 바이오 센서에서 좋은 감도를 가진다. 금 나노 막대(gold nanorod, AuNR)에서 플라즈몬 감쇠는 LSPR 선폭을 넓혀준다. 그 중 화학적 계면 감쇠(chemical interface damping, CID)는 플라즈몬 금 나노 입자에서 균일한 LSPR 선폭을 넓히는 주요 붕괴 과정 중 하나이지만 가장 잘 이해되지 않은 감쇠 메커니즘이다.

본 논문에서는 CID를 더 잘 이해하기 위해 단일 AuNR을 주사 전자 현미경(scanning electron microscope, SEM)과 암시야(dark-field, DF) 현미경을 이용한 연구를 수행하였다. 먼저, 25 nm의 고정 직경에서 3가지 다른 종횡비(aspect ratio, AR)를 갖는 단일 AuNR에서 균일한 LSPR 선폭의 크기에 따른 확장을 조사했다. LSPR 선폭은 표면으로의 hot electron의 평균 거리가 감소하기 때문에 단일 AuNR의 AR이 감소할수록 증가했다. 둘째, 단일 AuNR에 흡착된 thiol 분자가 균일한 LSPR 선폭에 미치는 영향을

조사했다. LSPR 선폭은 1-alkanethiol의 탄소사슬 길이가 증가함에 따라 넓어졌다. 셋째, 서로 다른 크기의 단일 AuNR에서 LSPR 선폭에 대한 주변 매질의 굴절률 변화의 영향을 조사하였다. LSPR 선폭은 매질의 유전상수가 증가하여도 거의 일정하게 유지되었다. 마지막으로 실제 생체 분자를 사용하여 CID 효과를 확인하기위한 연구를 수행했으며 biotinylated BSA 분자가 검출될 수 있음을 입증하였다.

Abstract

Among the metal nanoparticles, noble metal nanoparticles such as gold, silver, and copper have been applied in various fields due to their unique optical properties. In particular, gold nanoparticles (AuNP) have been studied extensively in the field of sensors based on localized surface plasmon resonance (LSPR). Of the various gold nanoparticles, rod-shaped particles have an anisotropic shape and thus have good sensitivity in a refractive index-based biosensor. In gold nanorods (AuNR), the plasmon attenuation broadens the LSPR linewidth. Among them, chemical interface damping (CID) is one of the major decay processes for widening the uniform LSPR linewidth in plasmonic gold nanoparticles, but it is the least understood damping mechanism.

In this paper, a single AuNR was studied using a scanning electron microscope (SEM) and a dark-field (DF) microscope to better understand the CID. First, we examined the extent of uniform LSPR linewidth in a single AuNR with three different aspect ratios (AR) at a fixed diameter of 25 nm. The LSPR linewidth increased as the AR of a single AuNR decreased as the average distance of hot electrons to the surface decreased. Second, the effect of thiol molecules adsorbed on a single AuNR on the uniform LSPR linewidth was investigated. The LSPR linewidth increased as the carbon chain length of 1-alkanethiol increased. Third, the influence of the change of the refractive index of the surrounding medium on the LSPR linewidth in a single AuNR of different sizes was investigated. The LSPR linewidth remained almost constant even when the dielectric constant of the medium

increased. Finally, we have conducted a study to investigate CID effects using real biomolecules, biotinylated BSA, and demonstrated that biotinylated BSA molecules can be detected based on the CID of single AuNRs.

Index

Figure index

I. Introduction

Plasmonic gold nanoparticles exhibit unique size- and shaped- dependent optical properties because of localized surface plasmon resonance (LSPR), which arises when the incident light is in resonance with the collective oscillation of the conducting electrons in the metallic nanoparticles.[1] Plasmon damping channels on gold nanoparticles are of great interest for their potential uses in photochemical processes and sensing experiments. So far, plasmon damping has been mainly studied by ultrafast spectroscopy techniques because of the smallest timescale for measuring the plasmon relaxation channel pathways. However, such ultrafast techniques are expensive and inconvenient to perform.[2] Fortunately, homogeneous plasmon spectrum linewidth measurements, using only single nanoparticles over the heterogeneous linewidth of an ensemble spectrum, enabled us to overcome the aforementioned timescale limitation.[3-5] Given the proportional relationship between the LSPR linewidth and the damping rate, the homogeneous LSPR linewidth, using far field single particle spectroscopy techniques, shows a detailed picture of the total LSPR decay pathways.[6]

So far, dark-field (DF) scattering microscopy and spectroscopy have been used to investigate the broadening of the homogeneous LSPR linewidth (or plasmon damping) in single gold nanoparticles by several groups.[4, 7-10] The LSPR linewidth is governed by lifetime broadening because of various plasmon decay processes, including bulk metal damping Γ_{bulk}, electron surface scattering Γ_{surf}, radiation

damping Γ_{rad}, and chemical interface damping (CID) Γ_{CID}.[5, 7-8, 11-15] Therefore, the LSPR total damping channel can be described by the following equation (1):

$$\Gamma_{tot} = \Gamma_{bulk} + \Gamma_{rad} + \Gamma_{surf} + \Gamma_{CID} \quad (1)$$

Although bulk damping is an intrinsic characteristic of a material, that is 73 meV for gold, the radiation, surface scattering and CID are functions of the volume of nanoparticles, the average distances of electrons to scatter on the surface and the chemical binding and electronic effects on the surface of the nanoparticles, respectively. Among these decay processes, CID is the recently proposed damping channel pathway. In the presence of strongly interacting adsorbate molecules, CID occurs and results in the direct transfer of plasmon-induced hot-electrons to the adsorbate's empty orbitals (LUMOs: lowest unoccupied molecular orbitals). To date, there have been few studies to reveal CID at the single particle level. Recent studies have utilized the homogeneous LSPR linewidth of single AuNRs. For example, Foerster et al. studied the size-dependent broadening of the homogeneous LSPR linewidth while changing the chemical environment of a single AuNR with a similar aspect ratio (AR).[11] They demonstrated that CID depends on the electrons reaching the surface, confirmed by the time evolution of the Langmuir adsorption model in surface chemistry together with the electrons' effective path length derived by Coronado and Schatz. Furthermore, in our previous study, we presented single

particle DF scattering studies to better understand the CID effect in single AuNRs with an AR of 3.[12]

Despite the aforementioned recent contributions to CID using single particle spectroscopy, our understanding on its mechanism in plasmonic gold nanoparticles is still limited and the question associated with its true nature remains elusive.[11] More specifically, our understanding of CID is still very limited in terms of three important aspects: (1) the effect of size while varying the length of AuNRs at a fixed diameter, (2) varying the adsorbate molecules on the surface of the nanoparticles, and (3) chemical interface damping of nanoparticles by adsorption of real biomolecules. In this regard, it is highly desirable to carry out single particle DF studies to gain deeper insights into CID in single AuNRs with various aspect ratios (ARs) and real-biological molecules.

In the present study, we carried out DF scattering measurements of AuNRs with three different ARs to better understand their optical properties at the single particle level. More specifically, we investigated how the particle size as well as the medium dielectric constant can affect the homogeneous LSPR linewidth in single AuNRs of different sizes and ARs at a fixed diameter. Furthermore, to better understand CID, we investigated the effect of various adsorbate molecules (1-alkanethiol with different carbon chain lengths and 4-nitrothiophenol with a strong electron withdrawing group) on the homogeneous LSPR linewidth of single AuNRs with different sizes. Finally, we investigated biomolecules, such as biotin and BSA, that are widely used as linkers or acceptors in gold nanoparticle-based biosensors.

Biotin with sulfur group is generally known as vitamin B7 and has been widely applied to biosensors due to its specific binding with streptavidin.[16-19] Serum albumin is one of the most commonly used protein models found in body fluids and in bio experiments. Therefore, we provide a deeper understanding of CID effect in AuNRs and demonstrate the possibility of using CID to detect real-biological molecules having sulfur group in AuNRs. The results will allow for the development of biosensors based on CID with AuNRs as well as biotinylated molecules.

II. Experimental

II-1. Materials

Citrate-stabilized AuNRs with three different ARs (25 nm × 47 nm, 25 nm × 60 nm, 23 nm × 74 nm) were purchased from Nanopartz (Loveland, CO, USA) and Sigma-Aldrich (St. Louis, MO, USA). All thiol molecules (1-butanethiol, 1-hexanethiol, 1-decanethiol, and 4-nitrothiophenol) used in this study were purchased from Sigma-Aldrich (St. Louis, MO, USA). Biotinylated Bovine Serum Albumin(biotin-BSA) was purchased from Thermo Fisher. Bovine Serum Albumin and biotin was purchased from Sigma Aldrich.

II-2. Sample Preparation and Characterization

Microscope cover glasses were cleaned by first sonicating in acetone for 15 min, and then in methanol for 15 min, followed by O_2 plasma cleaning for 1 min. The solution containing AuNRs was 10× diluted and sonicated for 3 min to prevent the aggregation of the nanoparticles. A drop of the diluted AuNR solution was then cast onto the aminosilanized glass slide and allowed to dry. In this study, a silane method with APTES allowed citrate-stabilized AuNRs to be immobilized on the glass slides. The concentration of AuNRs on the glass surface was controlled to be 1 μm^{-2} in order to facilitate single AuNR characterization and to minimize inter-particle LSPR coupling resulting in a spectral shift.

II-3. Characterization of Gold Nanorods

To evaluate the shapes and dimensions, characterization was carried out using a FEI Quanta ESEM2 SEM. Furthermore, heterogeneous LSPR ensemble absorption spectra in water were recorded with a Varian Cary 300 UV-Vis spectrometer.

II-4. Single Particle Microscopy and Spectroscopy

In a home-built system, dark-field (DF) microscopy imaging was carried out under a Nikon inverted microscope (ECLIPSE Ti-U). In the DF mode, the microscope was equipped with a Nikon Plan Fluor 100× 0.5–1.3 oil iris objective and a Nikon DF condenser. An Andor iXonEM+ CCD camera (iXon Ultra 897) was employed to record the DF images of AuNPs. The collected images were analyzed using ImageJ software. Furthermore, DF scattering spectra were acquired with an Andor spectrophotometer (SHAMROCK 303i, SR-303I-A) and an Andor CCD camera (Newton DU920P-OE). When obtaining a spectrum, the scanning stage moved the sample to the desired location so that only scattered light from the selected location was collected by the objective. The scattered light was directed to the entrance of the spectrophotometer, dispersed by a grating (300 l mm^{-1}, a center wavelength of 700 nm), and detected using a Newton CCD camera. The background was measured at a region without any particles. Data analysis was performed with

specially designed Matlab programs. The spectra were fitted to a Lorentzian function $I(\omega) = C_0/[(\omega - \omega_0)^2 + \Gamma^2/4]$ to determine the LSPR linewidth Γ and the resonance frequency ω_0.

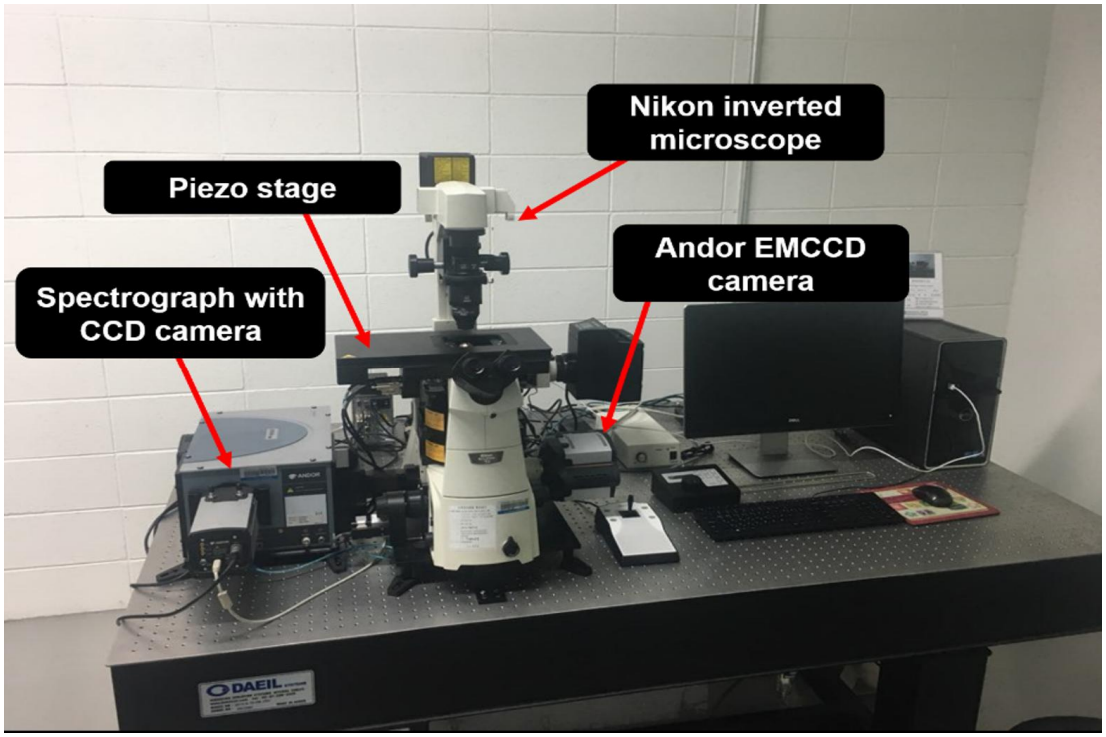

Fig. 1 Optical microscope system for single particle spectroscopy

III. Results and discussion

III-1. Size and Chemical Effects on Plasmon Damping at the Interface between Adsorbate and Anisotropic Gold Nanorods

AuNRs with three different ARs of 1.88, 2.40, and 3.22 at a fixed diameter ofB25 nm were purchased from Nanopartz (Loveland, CO, USA) and Sigma-Aldrich (St. Louis, MO, USA) (Fig. 2). Fig. 2A–C show the SEM images of AuNRs with different sizes. The extinction spectra of the AuNRs dispersed in water were collected with a Varian Cary 300 UV-Vis spectrophotometer (Fig. 2D). The transverse LSPR peak appeared at approximately 516 nm, while the longitudinal LSPR peak appeared in the spectral range of 650–750 nm for the AuNRs measured in this study. The longitudinal LSPR peak was redshifted upon increasing the AR from 1.88 to 3.22. However, homogeneous single particle measurements are necessary to have a deeper understanding of the optical properties of AuNRs without ensemble averaging.

In the present study, we performed DF scattering measurements of AuNRs with three different sizes at the single particle level. The sample was prepared by drop casting a solution containing AuNRs on a glass slide. In this study, citrate-stabilized AuNRs were immobilized on aminosilanized glass slides. Furthermore, the concentration of AuNRs on the glass surface was controlled to be about 1 μm^{-2} in order to facilitate single AuNR characterization and to minimize inter-particle LSPR coupling, resulting in a spectral shift. The diagram of the experimental arrangement

for DF scattering studies is depicted in Fig. 3.

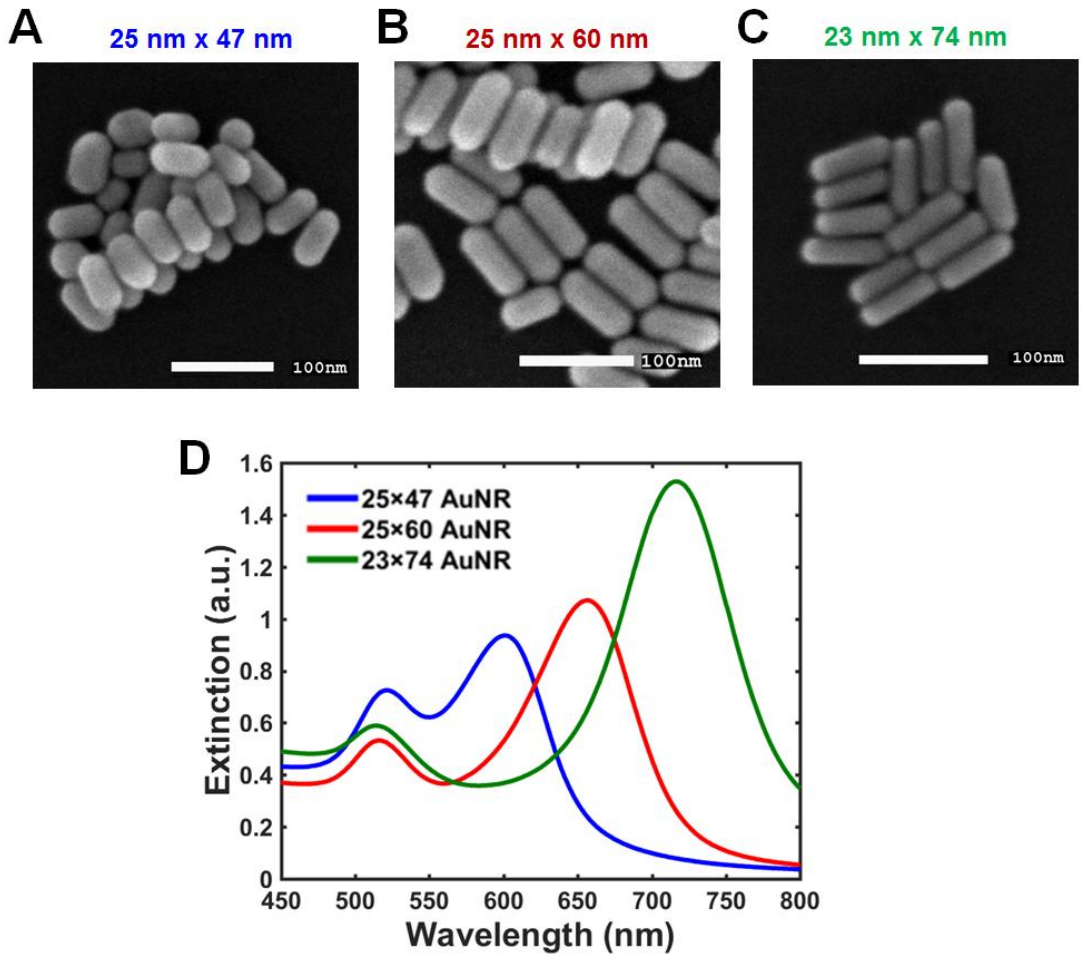

Fig. 2 (A–C) SEM images of single AuNRs with three different aspect ratios of 1.88, 2.40, and 3.22 at a fixed diameter of ~25 nm. (D) UV-Vis extinction spectra of the three-different AuNRs dispersed in water.

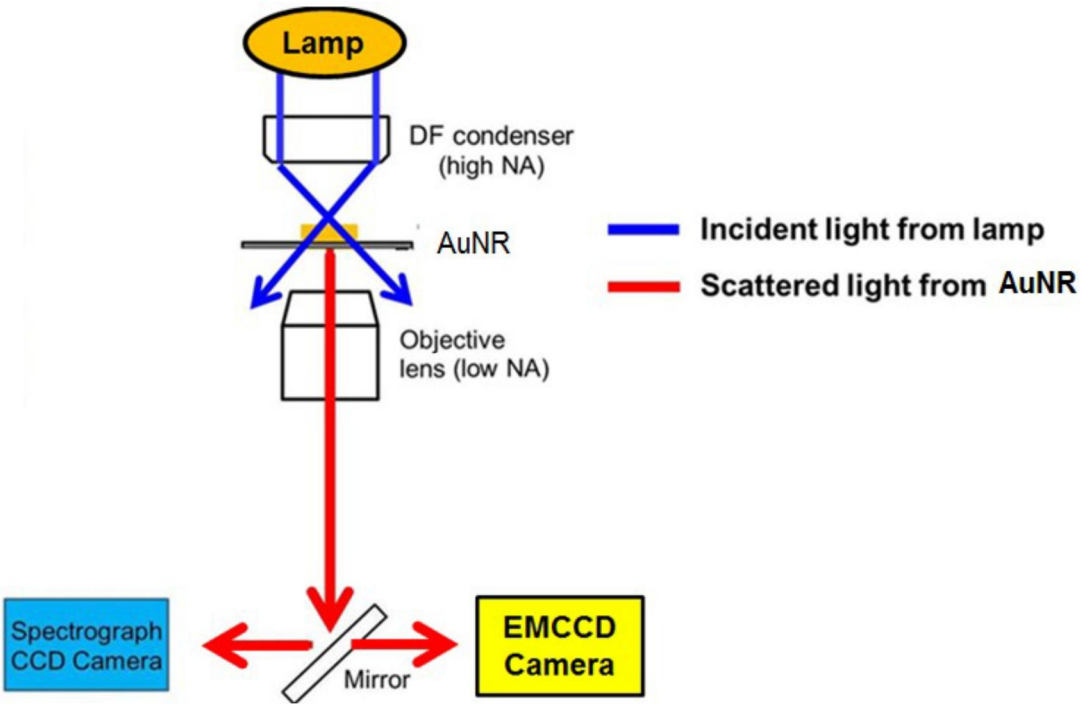

Fig. 3 Experimental setup for DF scattering microscopy and spectroscopy. The blue-line shows incident light from lamp, while the red-line indicates the scattered light from AuNR.

Fig. 4A shows a schematic to describe the working principle of a DF microscope, and only scattered light from the sample is collected using the objective lens. Fig. 4B shows a DF scattering image of single AuNRs with an AR of 3.22 (23 nm × 74 nm on average). We then attempted to obtain the scattering spectra of single AuNRs in order to have a deeper understanding of their optical properties at the single particle level. To obtain the scattering spectra of the AuNRs, we used the electronic scanning stage to move the sample to the desired location. Therefore, the scattered light from the selected location was directed to the entrance of the spectrometer combined with a CCD camera. Fig. 4C shows the scattering spectrum of AuNR1 indicated with a white square in Fig. 4B. We found that the scattering spectrum for AuNR1 in water peaked at around 716 nm corresponding to the longitudinal surface plasmon resonance, which is consistent with the ensemble spectrum in Fig. 2D.

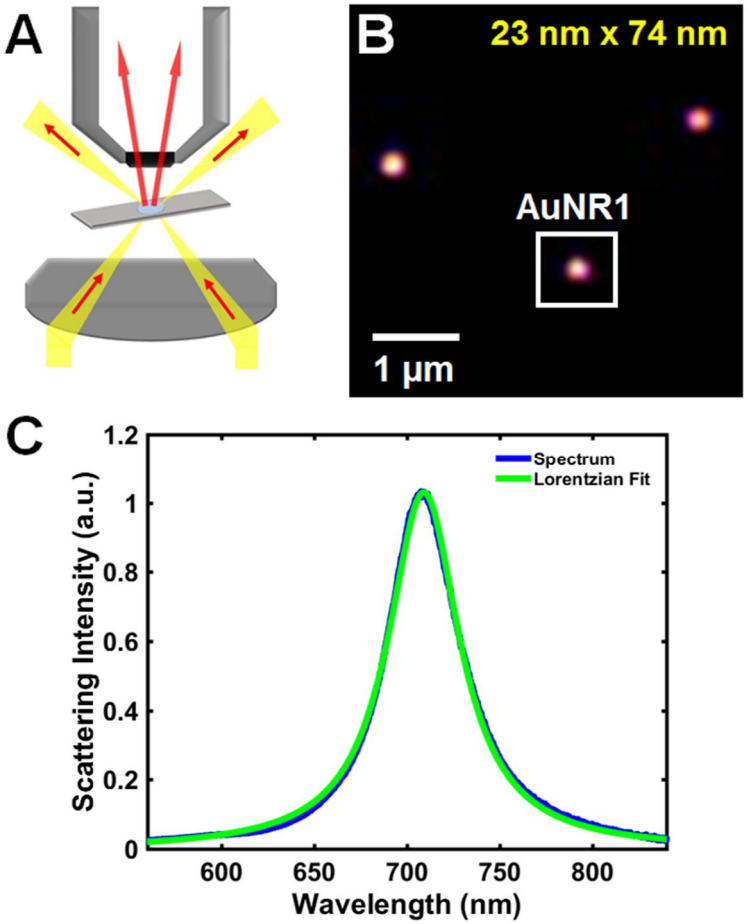

Fig. 4 (A) The working principle of DF microscopy. (B) DF scattering image of single AuNRs with an average size of 23 nm × 74nm. (C) Single particle scattering spectrum of AuNR1 indicated in (B). The longitudinal LSPR peak for the AuNR1 is observed at approximately 716 nm. The green curve shows a fit to Lorentzian function.

In a previous study, we investigated the broadening of the LSPR linewidth in single AuNRs with an AR of 3.[12] However, the effect of particle size on plasmon damping in single AuNRs is still poorly understood. In the present study, we investigated how particle size affects the LSPR linewidth of single AuNRs with different ARs. We obtained the scattering spectra of single AuNRs with different ARs of 1.88, 2.40, and 3.22 in water (Fig. 5A), which were then fitted with a Lorentzian function to calculate the homogeneous LSPR linewidth. As shown in Fig. 4C, the scattering spectra were well fitted with a Lorentzian function. The LSPR linewidth slightly increased upon decreasing the AR from 3.22 to 1.88 for single AuNRs measured in this study, while the LSPR wavelength increased upon increasing the AR (Fig. 5B). The increase in the LSPR linewidth for smaller AuNRs could be explained by the reduced average distance of photo-generated hot electrons to the nanoparticle surface, which is consistent with a previous study.[11]

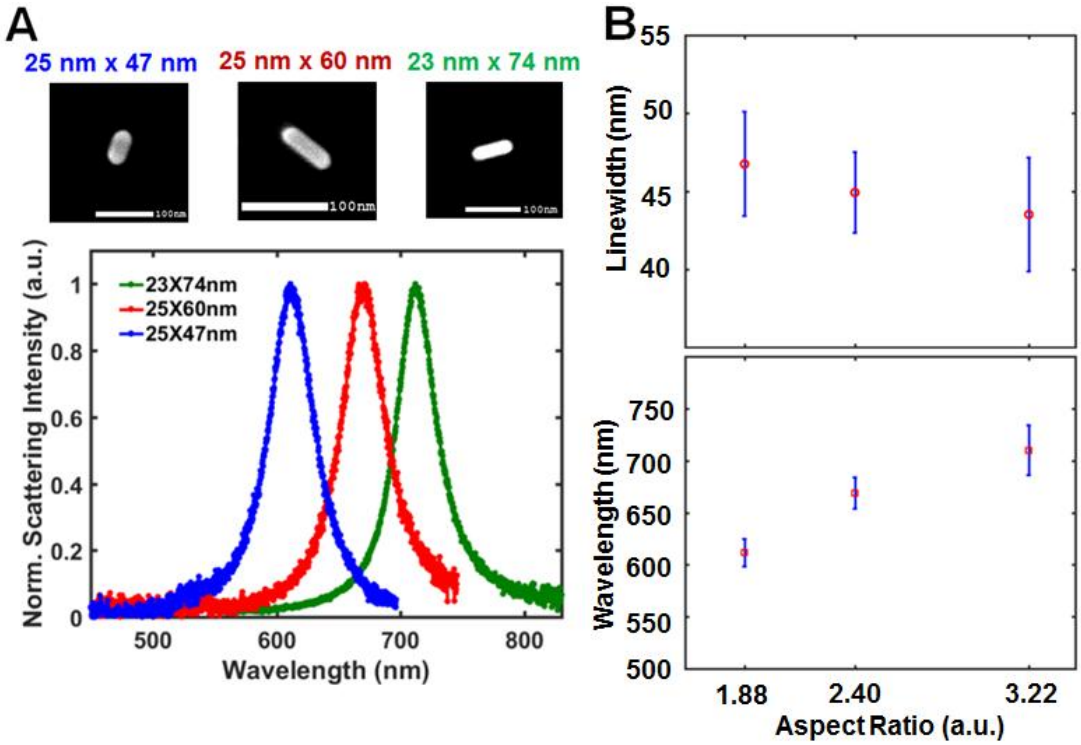

Fig. 5 (A) Scattering spectra of single AuNRs with different ARs of 1.88 (blue), 2.40 (red), and 3.22 (green). SEM images of single AuNRs measured in this study are also provided in (A). (B) Change in the SPR linewidth (up) and wavelength (bottom) as a function of AR from 1.88 to 3.22.

We further elucidated the effect of altering the refractive index of the surrounding medium on the LSPR linewidth in single AuNRs with different sizes. We obtained the scattering spectra of single AuNRs in three different environments (air, water, and oil). Fig. 6 shows the single particle scattering spectra of a AuNR with different ARs deposited on a glass coverslip and surrounded by air, water, and oil. The LSPR spectrum was then fitted with a Lorentzian function to calculate the LSPR linewidth.[12] As shown in Figs. 6A–C, the LSPR wavelength increased as the refractive index increased from air to oil (Figs. 6G–I). This trend for the LSPR wavelength as a function of refractive index is in agreement with previous reports. More importantly, we found that the LSPR linewidth remains almost constant as the refractive index increases for a single AuNR with three different ARs (Figs. 6D–F), which is consistent with our previous result from a single AuNR with an AR of 3.[12] To verify this, we further performed discrete dipole approximation (DDA) calculations[20-22] that account for retardation effects, such as radiation damping. We used DDSCAT to calculate the relative concentrations of scattering and absorption to the extinction spectra as a function of medium refractive index. The DDA calculations fully reproduced the experimental results (Figs. 7A–C), and the trend for the linewidth as a function of medium dielectric constant was in agreement with the DDA calculations. It was found that the LSPR wavelength increases with increasing medium refractive index and that the LSPR linewidth remains almost constant with increasing medium refractive index for single AuNRs with three different ARs of 1.88, 2.40, and 3.22. Therefore, we provide a better understanding on how the LSPR

linewidth of single AuNRs with different ARs (or sizes) is affected by the refractive index of the surrounding medium.

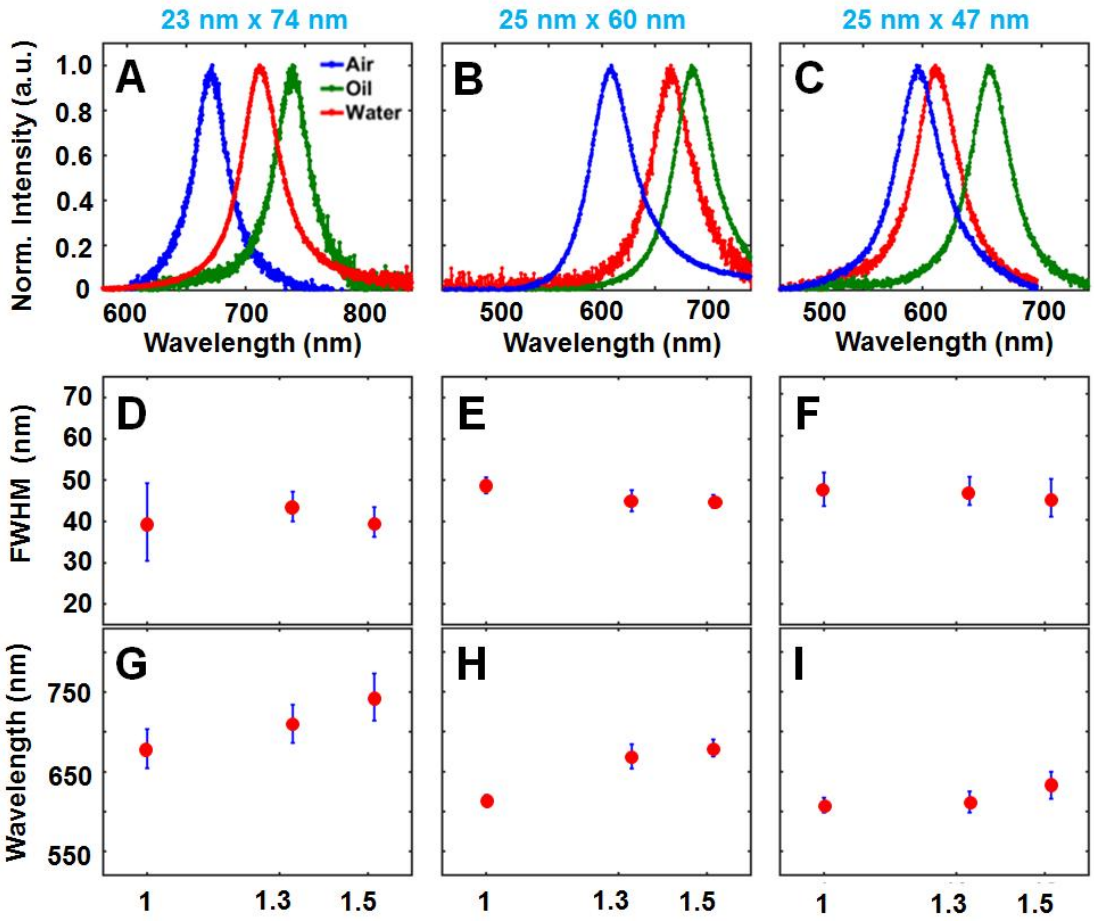

Fig. 6 (A, B, C) Scattering spectra of single AuNRs with three different ARs (1.88, 2.4, 3.22) in air (blue), water (red), and oil (green). (D, E. F) Change in the LSPR linewidth of single AuNRs with different ARs while varying the medium dielectric environment from air to oil. (G, H, I) Change in the LSPR wavelength of single AuNRs with different ARs while varying the medium dielectric environment from air to oil.

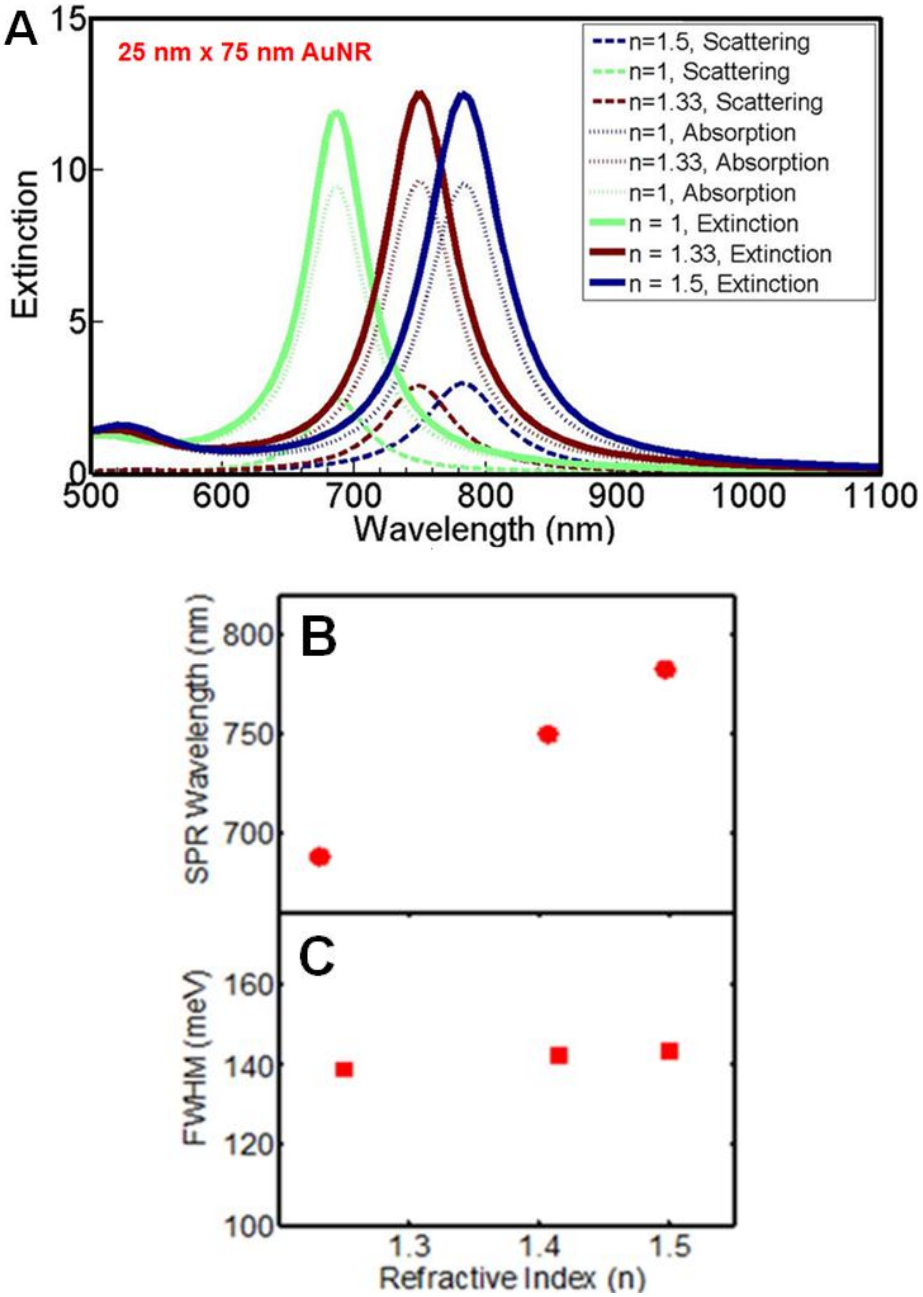

Fig. 7 (A) DDA calculation on the extinction, absorption, and scattering spectra of AuNR (25 nm ⅹ 75 nm) as a function of the medium refractive index (air, water, oil). (B) Change in the LSPR scattering wavelength in a different medium. (C) Change in the SPR linewidth as a function of refractive index from air to oil.

Besides the effect of refractive index on the LSPR linewidth, it is also important to elucidate the broadening of the LSPR linewidth caused by chemical interactions with AuNRs of different ARs. The broadening of the LSPR linewidth is intimately associated with the reduction of lifetime of surface plasmon excitation. However, this recently proposed CID effect on linewidth broadening is not well studied or understood, and simple models have been employed to investigate its influence on surface plasmon excitation.[13, 23-24] We therefore performed detailed studies on the chemical effects responsible for the broadening of the LSPR linewidth in single AuNRs, and the preferred and strong covalent soft–soft interactions between sulfur atoms and gold surfaces were used to investigate the CID effect in single AuNRs of different ARs. Fig. 8 shows the scattering spectra of an AuNR (AR: 3.22) in ethanol (red) and after adding 1 μM of 1-decanethiol in ethanol (blue). There was no remarkable structural change after modification of AuNRs with thiol molecules.[12, 25] As demonstrated in Fig. 8A and B, we observed that the thiol molecule causes both a red shift and a strong plasmon damping with a much increased LSPR linewidth. The change in the linewidth is better illustrated where the same spectra are normalized (Fig. 8B). The full width at half maximum (FWHM) values were 101 meV and 114 meV for the red and blue spectra, respectively. The increase in the LSPR linewidth was also observed for single AuNRs with different ARs of 1.88 and 2.4. Therefore, the increase in the LSPR linewidth can be attributed to specific interactions of the adsorbed thiol molecules with the LSPR oscillation. It is worth noting that both the red shift and the increase in the LSPR linewidth caused

by the chemical effect of adsorbate are not related as illustrated in Fig. 9. The former is related to the refractive index changes by the adsorbate molecule and independent of the latter which is due to specific interactions of the adsorbed molecules that lead to a reduction in the lifetime of surface plasmon excitation.[15, 26]

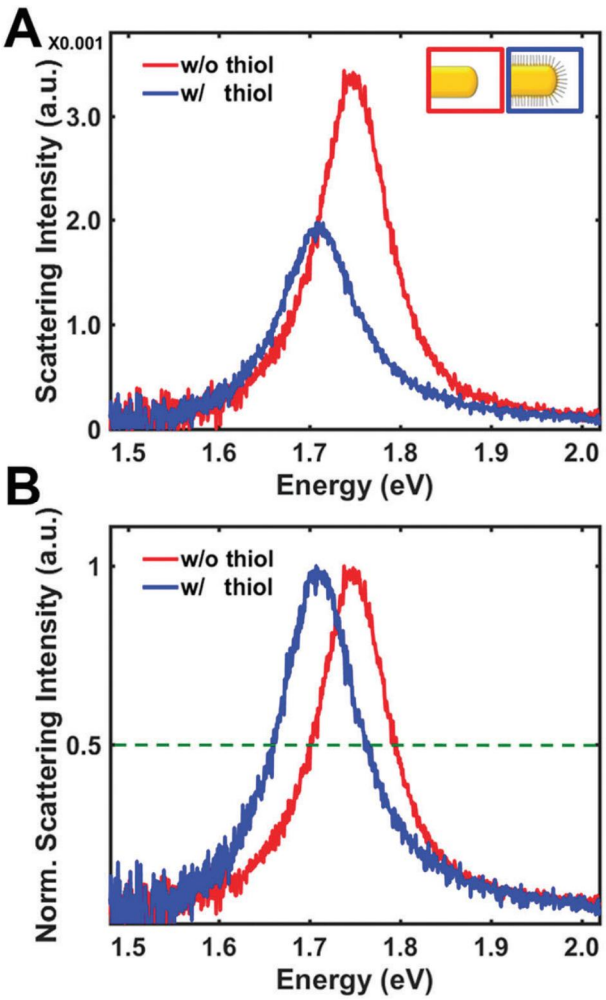

Fig. 8 (A) Single AuNR (23 nm x 74 nm) scattering spectra in ethanol (red) and after adding 1-decanethiol (1 mM) in ethanol (blue). The scattering spectrum is red-shifted and strongly damped with an increased linewidth. (B) The change in the LSPR linewidth is better illustrated where the same spectra are normalized.

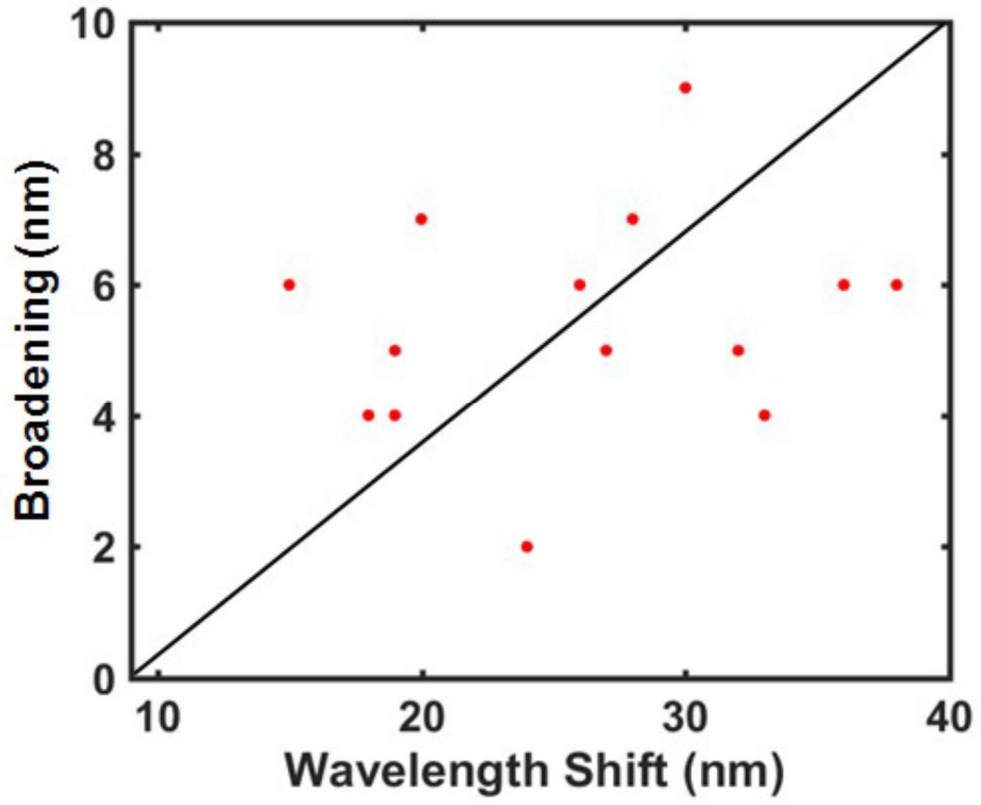

Fig. 9 Linear illustration of the non-dependence character of the of the redshift caused by the refractive index change and the broadening of the full width at half maximum caused by the retardation of decay time due to the interaction of adsorbate with AuNR surfaces.

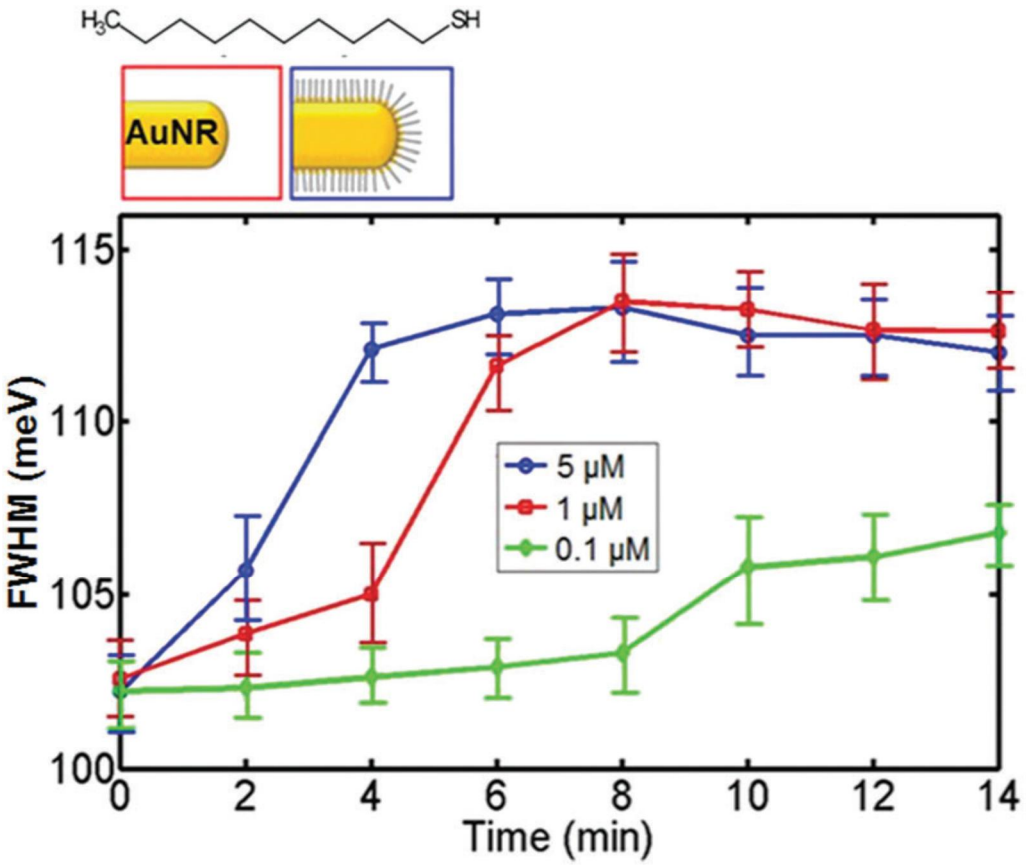

Fig. 10 Change in the LSPR linewidth induced by the adsorption of thiol molecules on the surface of AuNRs with an average size of 23 nm × 74 nm. The scattering spectra of the AuNRs deposited on a glass substrate were obtained as a function of time after adding 1-decanethiol with different concentrations of 0.1 mM (green), 1 mM (red), and 5 mM (blue) in ethanol.

Although the LSPR redshift effect due to the change in the refractive index is independent of the LSPR broadening, the refractive index in the surrounding AuNRs is strongly dependent on the layers (concentration) or saturation conditions of interacting adsorbate molecules. Further, it was shown that the CID effect can be reduced by decreasing the number of molecules (concentration) on the surface of nanoparticles.[15] Therefore, to control both effects, we have to fix an optimized concentration on the surfaces of AuNRs. To optimize the effect of layers or saturation conditions on the surface of AuNRs, the real time experiments were carried out at various concentrations to determine the concentration and the corresponding time at which the broadening, that is CID, is kept unchanged. Under such conditions we maximally and effectively observed the linewidth due to specific interactions of adsorbates. Fig. 10 shows the effect of the concentration of thiol on the LSPR linewidth during a chemical reaction on the surface of single AuNRs (23 nm x 74 nm) in real time. We varied the concentration of 1-decanethiol from 0.1 μM to 5 μM. Obviously, the LSPR linewidth was rapidly increased at a concentration of 5 μM, while it was slowly increased at a concentration of 0.1 μM. Two concentrations of adsorbate, 1 μM and 5 μM showed the highest LSPR linewidth after 8minutes. It should be noted that the change in the LSPR linewidth in this study is only ascribed to the adsorption of thiol molecules on the AuNRs. Therefore, under our experimental conditions, the layer on the surface was assumed to be uniform at the concentration and time values that correspond to the maximum linewidth. We then used 1 μM as the concentration of the adsorbate for a time higher than 8 minutes

for all experiments.

As a next step, we further investigated the effect of varying adsorbate thiol molecules on the LSPR linewidth of single AuNRs with different ARs, which has been largely unanswered so far. We therefore tried to elucidate the CID effect using various 1-alkanethiol molecules with different carbon chain lengths. In this study, we used three kinds of 1-alkanethiol molecules, 1-butanethiol, 1-hexanethiol, and 1-decanethiol. Fig. 11A shows the normalized scattering spectra of single AuNRs with an AR of 2.4 (25 nm × 60 nm) after chemical adsorption in ethanol. The LSPR linewidth increased with increasing the number of carbons from 4 to 10 in single AuNRs. To further verify this trend with statistical analysis, we measured many single AuNRs with different ARs. We found that the LSPR linewidth increased with increasing the carbon number for single AuNRs of different sizes (Fig. 11B). Furthermore, single AuNRs with a smaller AR induced a larger broadening in the LSPR linewidth for 1-alkanethiol molecules (Fig. 11B). This indicates that single AuNRs with a smaller AR show higher sensitivity to adsorbate molecules in terms of CID-induced LSPR linewidth broadening.

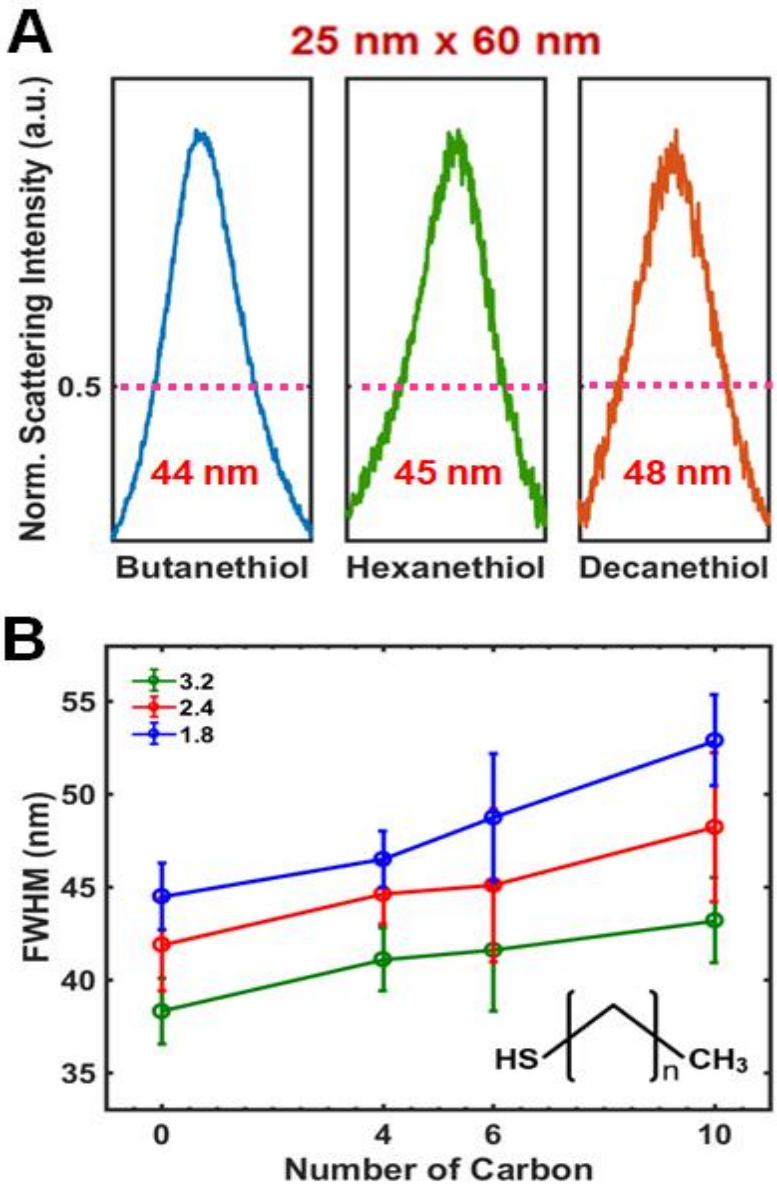

Fig. 11 (A) Normalized scattering spectra of single AuNRs (25 nm x 60 nm) at various 1-alkanethiol molecules in ethanol (RI = 1.36) with different chain lengths (1-butanethiol, 1-hexanethiol, and 1-decanethiol). We used 1μM as the concentration of adsorbate molecules. (B) Changes in the FWHM in single AuNRs with different ARs (1.88, 2.40, and 3.22) as a function of carbon number in 1-alkanethiol.

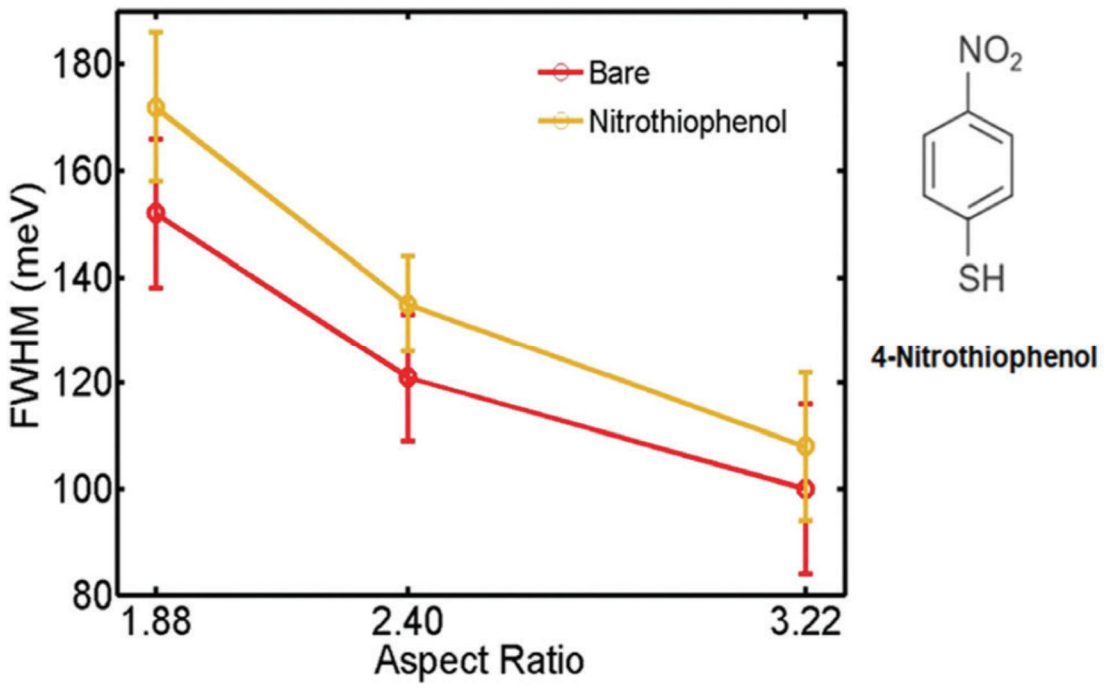

Fig. 12 Changes in the FWHM in single AuNRs with different ARs (1.88, 2.40, and 3.22) in the presence of 4-nitrothiophenol with strong EWGs (orange curve).

By further examining the results in Fig. 11B, we can easily observe for the same given chain length that the increase of broadening is highly pronounced with respect to the smallest of the nanoparticles than for an increase in the chain length of 1-alkanethiol. This indicates that for CID, the molecular orbital binding effect enhances the surface contact effects and accordingly affects the LSPR damping to a large extent for small Au nanoparticles. As the size decreases, the surface of contact (or overlapping) between gold and adsorbates' sulfur atoms increases and the broadening can become even larger for smaller AuNRs due to the transfer of hot electron energies from gold to adsorbates.

Besides the linear alkanethiol molecules, we further investigated the interfacial electronic effect of adsorbates with the benzene ring bound on the Au surface. In this study, we employed 4-nitrothiophenol (4-NTP) with a very strong electron withdrawing group (EWG) as the adsorbate. As shown in Fig. 6, 4-NTP induced a larger broadening in the LSPR linewidth for AuNRs. This can be explained by the fact that EWG could more significantly reduce the effective distance of plasmon-induced hot-electron transfer from the Au metal during the direct interfacial hot-electron transfer or CID. Furthermore, it should be noted that AuNRs with smaller ARs resulted in a larger LSPR broadening of the LSPR linewidth, which is consistent with the result shown in Fig. 11 for 1-alkanethiol. Therefore, we found that CID arises more effectively in the case of AuNRs with smaller ARs at a fixed diameter and adsorbate thiol-molecules with strong EWGs.

III-2. Plasmonic Sensing of Biotin-BSA Proteins by Chemical Interface Damping of Single Gold Nanorods

We investigated the broadening of LSPR linewidth induced by the adsorption of real-biological molecules. In this study, biotinylated BSA was selected as the target molecule. The reason to select biotin in this study is that it has a sulfur group than can withdraw electrons from gold nanoparticles and induced CID phenomenon, just like thiol groups.[16] After the AuNR surface was modified with biotin-BSA (Fig. 13A), the scattering spectrum of a single particle was measured using a DF microscope. In comparison with bare AuNR, the scattering intensity of AuNR with biotin-BSA was significantly reduced and the LSPR wavelength region was redshifted by ~70 nm Furthermore, FWHM is broadened by 10 nm in AuNR with biotin-BSA. Therefore, it was confirmed that CID due to chemical bonding of AuNR and biotin-BSA occurred and broadening of LSPR linewidth occurred. This demonstrates the ability to detect biotin-BSA through the increase in the LSPR linewidth as a result of experiments using biomolecules with sulfur groups.

Biotinylated BSA studies confirmed the increase of linewidths due to CID effects. Therefore, the same experiment was performed using BSA molecules and biotin as control experiments. In Fig. 14, when BSA molecules were attached only to AuNR, the peak shifted from 710 nm to 760 nm as the local refractive index changes. However, when the BSA molecules are adsorbed on the gold surface, there was no broadening in FWHM. In case of biotin with sulfur, LSPR peak shifted as BSA, but FWHM was also increased by 7 nm. Therefore, we found that BSA molecules not

containing biotin cannot induce the CID effect, while biotin can induce the CID due to the covalent bonding between sulfur and gold (Fig. 13B). As shown in Fig. 13B, biotin causes a broadening of the LSPR linewidth due to the CID effect because -S can make a bonding to the surface of the AuNR.

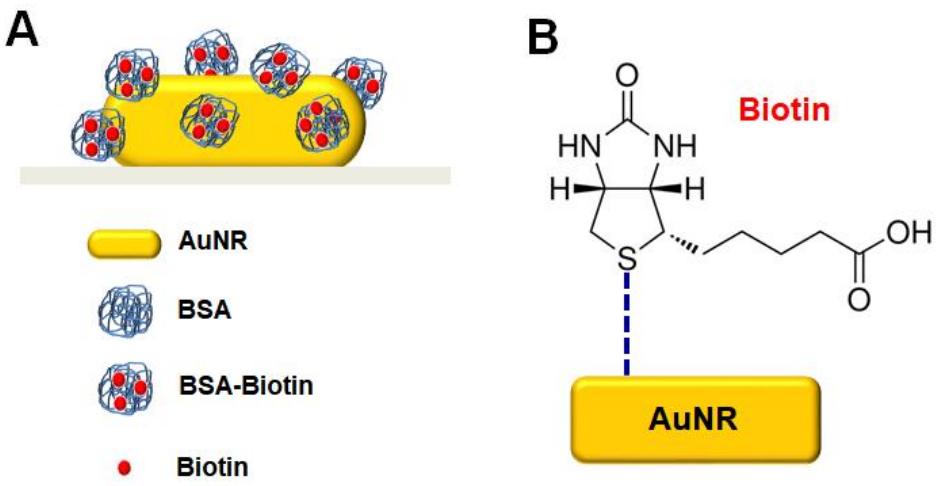

Fig. 13 (A) Single AuNRs are functionalized biotinylated BSA (B) Sulfur binding of biotin on gold nanoparticle surface.

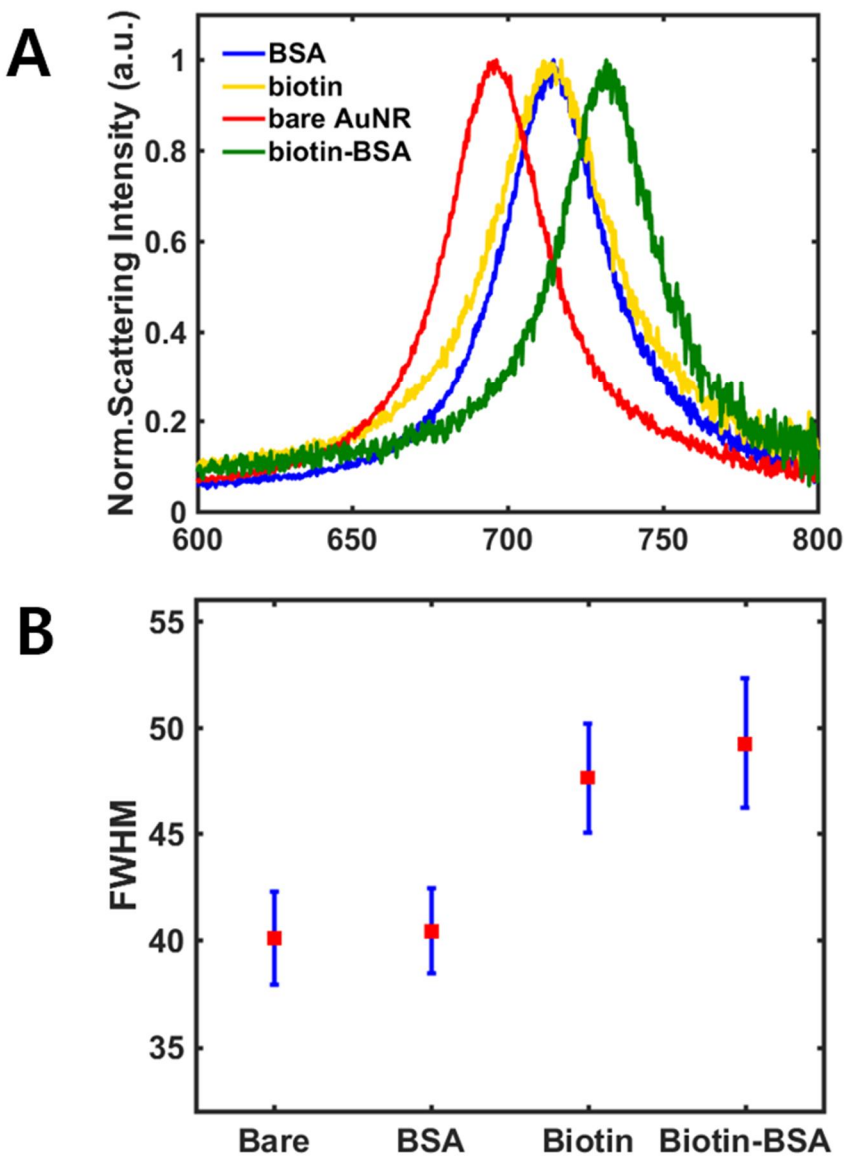

Fig. 14 (A) Normalized scattering intensity spectra. The target molecule adsorbed on the surface of the gold nanoparticles, resulting in peak shift. (B) Full width at half maximum change by target molecule (BSA, biotin, biotin-BSA)

IV. Conclusions

In summary, we performed DF scattering studies of single AuNRs with different sizes to deepen our understanding of size effect on plasmon damping including CID. First, we examined the size-dependent broadening of the homogeneous LSPR in single AuNRs with three different ARs at a fixed diameter of 25 nm. Single AuNRs with smaller ARs induced a larger broadening in the LSPR linewidth, which can be ascribed to the reduced average distance of hot electrons to the surface. Second, we investigated the effect of the refractive index variation of the surrounding medium on the LSPR linewidth in single AuNRs of three different sizes. The LSPR linewidth in single AuNRs remained almost constant regardless of their sizes while increasing the dielectric constant of the medium. Third, we examined the size effect on the CID of single AuNRs with adsorbate thiol molecules in ethanol. Single AuNRs with smaller ARs showed a larger broadening in the LSPR linewidth in the presence of adsorbate thiol molecules through CID. Therefore, the results enable us to better understand the size effect on plasmon damping including CID in single AuNRs. Finally, we investigated the effect of CID on the real biomolecules attached to AuNR surface. Only the biomolecule containing sulfur makes a chemical bond with AuNR and it increased the FWHM through the CID effect. Therefore, the results enable us to better understand the size effect on plasmon damping including CID in single AuNR. It also showed the possibility of CID-based biosensor.

V. Reference

1. S. L.; El-Sayed, M. A., OPTICAL PROPERTIES AND ULTRAFAST DYNAMICS OF METALLIC NANOCRYSTALS. *Annual Review of Physical Chemistry* **2003,** *54* (1), 331-366.

2. Pelton, M.; Liu, M.; Park, S.; Scherer, N. F.; Guyot-Sionnest, P., Ultrafast resonant optical scattering from single gold nanorods: Large nonlinearities and plasmon saturation. *Physical Review B* **2006,** *73* (15), 155419.

3. Hoggard, A.; Wang, L.-Y.; Ma, L.; Fang, Y.; You, G.; Olson, J.; Liu, Z.; Chang, W.-S.; Ajayan, P. M.; Link, S., Using the Plasmon Linewidth To Calculate the Time and Efficiency of Electron Transfer between Gold Nanorods and Graphene. *ACS Nano* **2013,** *7* (12), 11209-11217.

4. Novo, C.; Gomez, D.; Perez-Juste, J.; Zhang, Z.; Petrova, H.; Reismann, M.; Mulvaney, P.; Hartland, G. V., Contributions from radiation damping and surface scattering to the linewidth of the longitudinal plasmon band of gold nanorods: a single particle study. *Physical Chemistry Chemical Physics* **2006,** *8* (30), 3540-3546.

5. Sönnichsen, C.; Franzl, T.; Wilk, T.; von Plessen, G.; Feldmann, J.; Wilson, O.; Mulvaney, P., Drastic Reduction of Plasmon Damping in Gold Nanorods. *Physical Review Letters* **2002,** *88* (7), 077402.

6. Olson, J.; Dominguez-Medina, S.; Hoggard, A.; Wang, L.-Y.; Chang, W.-S.; Link, S., Optical characterization of single plasmonic nanoparticles. *Chemical Society Reviews* **2015,** *44* (1), 40-57.

7. Hu, M.; Chen, J.; Marquez, M.; Xia, Y.; Hartland, G. V., Correlated Rayleigh Scattering Spectroscopy and Scanning Electron Microscopy Studies of Au− Ag Bimetallic Nanoboxes and Nanocages. *The Journal of Physical Chemistry C* **2007,** *111* (34), 12558-12565.

8. Hu, M.; Petrova, H.; Sekkinen, A. R.; Chen, J.; McLellan, J. M.; Li, Z.-Y.; Marquez, M.; Li, X.; Xia, Y.; Hartland, G. V., Optical Properties of Au−Ag Nanoboxes Studied by Single Nanoparticle Spectroscopy. *The Journal of Physical*

Chemistry B **2006,** *110* (40), 19923-19928.

9. Nehl, C. L.; Grady, N. K.; Goodrich, G. P.; Tam, F.; Halas, N. J.; Hafner, J. H., Scattering Spectra of Single Gold Nanoshells. *Nano Letters* **2004,** *4* (12), 2355-2359.

10. Wang, X.; Zhang, Z.; Hartland, G. V., Electronic Dephasing in Bimetallic Gold−Silver Nanoparticles Examined by Single Particle Spectroscopy. *The Journal of Physical Chemistry B* **2005,** *109* (43), 20324-20330.

11. Foerster, B.; Joplin, A.; Kaefer, K.; Celiksoy, S.; Link, S.; Sönnichsen, C., Chemical interface damping depends on electrons reaching the surface. *ACS nano* **2017,** *11* (3), 2886-2893.

12. Ha, J. W., Chemical interface damping of single gold nanorods with low sensitivity to the medium dielectric constant. *Chemical Physics Letters* **2017,** *676*, 65-69.

13. Ha, J. W.; Sun, W.; Stender, A. S.; Fang, N., Dual-wavelength detection of rotational diffusion of single anisotropic nanocarriers on live cell membranes. *The Journal of Physical Chemistry C* **2012,** *116* (4), 2766-2771.

14. Zhang, Y.; He, S.; Guo, W.; Hu, Y.; Huang, J.; Mulcahy, J. R.; Wei, W. D., Surface-plasmon-driven hot electron photochemistry. *Chemical reviews* **2017,** *118* (6), 2927-2954.

15. Zijlstra, P.; Paulo, P. M.; Yu, K.; Xu, Q. H.; Orrit, M., Chemical Interface Damping in Single Gold Nanorods and Its Near Elimination by Tip Specific Functionalization. *Angewandte Chemie* **2012,** *124* (33), 8477-8480.

16. Laborde, H. M.; Lima, A. M. N.; Loureiro, F. C. C. L.; Thirstrup, C.; Neff, H., Adsorption, kinetics and biochemical interaction of biotin at the gold–water interface. *Thin Solid Films* **2013,** *540*, 221-226.

17. Raschke, G.; Kowarik, S.; Franzl, T.; Sönnichsen, C.; Klar, T. A.; Feldmann, J.; Nichtl, A.; Kürzinger, K., Biomolecular Recognition Based on Single Gold Nanoparticle Light Scattering. *Nano Letters* **2003,** *3* (7), 935-938.

18. Nusz, G. J.; Marinakos, S. M.; Curry, A. C.; Dahlin, A.; Höök, F.; Wax, A.; Chilkoti, A., Label-Free Plasmonic Detection of Biomolecular Binding by a Single Gold Nanorod. *Analytical Chemistry* **2008,** *80* (4), 984-989.

19. Scott, A. W.; Garimella, V.; Calabrese, C. M.; Mirkin, C. A., Universal Biotin–PEG-Linked Gold Nanoparticle Probes for the Simultaneous Detection of Nucleic Acids and Proteins. *Bioconjugate Chemistry* **2017,** *28* (1), 203-211.

20. Brioude, A.; Jiang, X.; Pileni, M., Optical properties of gold nanorods: DDA simulations supported by experiments. *The Journal of Physical Chemistry B* **2005,** *109* (27), 13138-13142.

21. Félidj, N.; Aubard, J.; Lévi, G., Discrete dipole approximation for ultraviolet–visible extinction spectra simulation of silver and gold colloids. *The Journal of chemical physics* **1999,** *111* (3), 1195-1208.

22. Yang, W. H.; Schatz, G. C.; Van Duyne, R. P., Discrete dipole approximation for calculating extinction and Raman intensities for small particles with arbitrary shapes. *The Journal of chemical physics* **1995,** *103* (3), 869-875.

23. Douglas-Gallardo, O. A.; Berdakin, M.; Sánchez, C. n. G., Atomistic insights into chemical interface damping of surface plasmon excitations in silver nanoclusters. *The Journal of Physical Chemistry C* **2016,** *120* (42), 24389-24399.

24. Persson, B., Polarizability of small spherical metal particles: influence of the matrix environment. *Surface Science* **1993,** *281* (1-2), 153-162.

25. Takahashi, H.; Niidome, T.; Kawano, T.; Yamada, S.; Niidome, Y., Surface modification of gold nanorods using layer-by-layer technique for cellular uptake. *Journal of Nanoparticle Research* **2008,** *10* (1), 221-228.

26. Tsalu, P. V.; Kim, G. W.; Hong, J. W.; Ha, J. W., Homogeneous Localized Surface Plasmon Resonance Inflection Points for Enhanced Sensitivity and Tracking Plasmon Damping in Single Gold Bipyramids. *Nanoscale* **2018**.